

Freeze-Fracture Electron Microscopy for Extracellular Vesicle Analysis

Nataša Resnik¹, Rok Romih¹, Mateja Erdani Kreft¹, Samo Hudoklin¹

¹ Faculty of Medicine, Institute of Cell Biology, University of Ljubljana

Corresponding Author

Samo Hudoklin

samo.hudoklin@mf.uni-lj.si

Citation

Resnik, N., Romih, R., Kreft, M.E., Hudoklin, S. Freeze-Fracture Electron Microscopy for Extracellular Vesicle Analysis. *J. Vis. Exp.* (187), e63550, doi:10.3791/63550 (2022).

Date Published

September 16, 2022

DOI

10.3791/63550

URL

jove.com/video/63550

Abstract

Extracellular vesicles (EVs) are membrane-limited structures released from the cells into the extracellular space and are implicated in intercellular communication. EVs consist of three populations of vesicles, namely microvesicles (MVs), exosomes, and apoptotic bodies. The limiting membrane of EVs is crucially involved in the interactions with the recipient cells, which could lead to the transfer of biologically active molecules to the recipient cells and, consequently, affect their behavior. The freeze-fracture electron microscopy technique is used to study the internal organization of biological membranes. Here, we present a protocol for MV isolation from cultured cancerous urothelial cells and the freeze-fracture of MVs in the steps of rapid freezing, fracturing, making and cleaning the replicas, and analyzing them with transmission electron microscopy. The results show that the protocol for isolation yields a homogenous population of EVs, which correspond to the shape and size of MVs. Intramembrane particles are found mainly in the protoplasmic face of the limiting membrane. Hence, freeze-fracture is the technique of choice to characterize the MVs' diameter, shape, and distribution of membrane proteins. The presented protocol is applicable to other populations of EVs.

Introduction

Extracellular vesicles (EVs) are membrane-limited vesicles released from cells into the extracellular space. The three main populations of EVs are exosomes, microvesicles (MVs), and apoptotic bodies, which differ in their origin, size, and molecular composition^{1,2,3}. The composition of EVs reflects the molecular profile of the donor cell and its physiological status (i.e., healthy or diseased)^{4,5}. This gives EVs immense potential in the diagnosis, prognosis, and therapy of human

diseases, and they have promising medical applications for the use in personalized medicine^{6,7,8}.

EVs are mediators of intercellular communication. They contain biologically active proteins, lipids, and RNAs, which interfere with biological processes in the recipient cell and can change its behavior^{9,10}. However, the composition of the

EV limiting membrane is crucial for the interaction with the recipient cell membrane.

The sources of EVs are body fluids and conditioned culture media. To isolate an EV population, a suitable isolation technique must be used. For example, centrifugation at $10,000 \times g$ yields a fraction enriched in MVs, whereas centrifugal forces of $\geq 100,000 \times g$ yield a fraction enriched in exosomes^{11,12}. The isolated fraction of EVs must be validated in terms of purity, size, and shape. For that purpose, the International Society for Extracellular Vesicles 2018 recommended three classes of high-resolution imaging techniques: electron microscopy, atomic force microscopy, and light microscopy-based super-resolution microscopy¹³. None of these techniques can provide information on the EV membrane interior.

Freeze-fracture electron microscopy is a technique of breaking frozen specimens to reveal their internal structures, particularly giving a view of the membrane interior. The steps of sample preparation are (1) rapid freezing, (2) fracturing, (3) making the replica, and (4) cleaning the replica¹⁴. In step 1, the sample is (optionally) chemically fixed, cryoprotected with glycerol, and frozen in liquid freon. In step 2, the frozen specimen is fractured in a freeze-fracture unit, which exposes the interior of the membrane bilayer. In step 3, the exposed fractured faces are shadowed with platinum (Pt) and carbon (C) to produce replicas. In step 4, the organic material is removed. The replica is analyzed in the transmission electron microscope (TEM). For accurate interpretation of the micrographs, one must follow guidelines for their proper orientation^{14,15}. Briefly, the direction of shadows in the micrograph is a reference to orientate the micrograph (i.e., to determine the direction of Pt shadowing) and, consequently, to determine convex and concave shapes (**Figure 1**). Two

interior views termed fractured faces of the membrane bilayer can be seen as a result of splitting the membrane by freeze-fracturing: the protoplasmic face (P-face) and the exoplasmic face (E-face). The P-face represents the membrane leaflet adjacent to the cell protoplasm, while the E-face represents the membrane leaflet adjacent to the extracellular space. Integral membrane proteins and their associations are seen as protruding intramembrane particles^{14,15}.

Here, the goal is to apply the freeze-fracture technique to characterize MVs in terms of size, shape, and the structure of their limiting membrane. Here, we present a protocol for the isolation and freeze-fracturing of MVs originating from human invasive bladder cancerous urothelial cells.

Protocol

1. Culturing cancerous urothelial cells and isolation of EVs

NOTE: A protocol to obtain EVs from a human invasive bladder cancer urothelial (T24) cell line is presented. However, culturing conditions have to be optimized to use other cell types.

1. Plate T24 cells with a density of 3×10^4 cells/cm² in three flasks (growing surface of 75 cm²) and start with culturing the cells in a CO₂ incubator for 3 days at 37 °C and a 5% CO₂ (**Figure 2A**).
1. Use a culture medium for T24 cells in a 1:1 (v/v) mixture of A-DMEM and F12 supplemented with 5% fetal bovine serum (FBS), 4 mM Glutamax, 100 mg/mL streptomycin, and 100 U/mL penicillin.

NOTE: The following isolation yields EVs enriched in MVs. Before starting the isolation, inspect the cells with a light microscope to confirm viability and

confluence (**Figure 2B**). Start collecting the EVs from the conditioned culture media when the T24 cells are at 70% confluence.

2. Collect the culture medium with MVs with a pipette from flasks (T75) into conical centrifuge tubes (**Figure 2C**). Centrifuge at $300 \times g$ for 10 min at 4°C (**Figure 2D**).
3. Carefully collect the supernatant into a new centrifuge tube with the pipette (**Figure 2E**).
4. Centrifuge the supernatant at $2,000 \times g$ for 20 min at 4°C .
5. Carefully collect the supernatant with the pipette into a new centrifuge tube.
6. Centrifuge at $10,000 \times g$ for 40 min at 4°C . Look for the presence of a whitish pellet at the bottom of the tube.
NOTE: If necessary, change the centrifuge rotor to reach the required g-force. The EV pellet is seen as a white pellet at the bottom of the centrifuge tube (**Figure 2F**); mark its location to avoid losing the pellet during pipetting (**Figure 2G**).
7. Carefully discard the supernatant with a pipette. To the pellet, add 1.5 mL of PBS and resuspend the pellet containing MVs. Put the suspension into a new centrifuge tube.
8. Centrifuge at $10,000 \times g$ for 40 min at 4°C and look for the presence of a white pellet at the bottom of the tube.
NOTE: The EV pellet is seen as a white patch at the bottom of the centrifuge tube; mark its location to avoid losing the pellet during pipetting.
9. Carefully discard the supernatant with a pipette. Gently add the fixative, 2.5% glutaraldehyde in 0.1 M sodium cacodylate buffer (pH 7.2). Leave for 20 min at 4°C (**Figure 2H**).

CAUTION: Glutaraldehyde and sodium cacodylate are toxic. Work in a fume hood, wear protective gloves, and discard them appropriately.

10. Carefully remove the fixative with a pipette. Add washing buffer (0.1 M sodium cacodylate buffer) to the pellet. Leave for 10 min at 4°C without resuspending the pellet.

2. Freezing of EVs

NOTE: Before freezing, first cryoprotect the samples with glycerol.

1. Prepare 0.1 M sodium cacodylate buffer. Remove the washing buffer and add 50 μL of 30% glycerol in 0.1 M cacodylate buffer. Gently resuspend the EVs to make the solution homogeneous. Incubate for 30 min at 4°C .
2. Clean the copper carriers with a central pit in the ultrasonic bath with chloroform for 5 min (**Figure 3A**). Air dry them and mark them with colors if using multiple samples (**Figure 3B**). Until use, keep the carriers in a dry, clean place (e.g., on lens paper in a Petri dish). Do not touch the carriers with bare hands.
 1. Prepare pipettes, solutions, filter paper, tweezers, a stereomicroscope, a Dewar flask with freon and liquid nitrogen (LN_2), a metal rod, and cryovials. Cool it down with LN_2 .
CAUTION: Wear protective equipment and work accordingly when handling LN_2 and cooled freon.
3. Resuspend the EVs again before freezing. Avoid the formation of air bubbles.
NOTE: Perform steps 2.4-2.7 rapidly.
4. Work under a stereomicroscope (**Figure 3C**). Transfer 1.5-1.7 μL of the sample into the central pit of the copper carrier to make a convex drop reaching higher than the

copper carrier edge while not spilling the sample over the edge (**Figure 3D**). In case of overspill, use filter paper to dry the outer ring of the carrier.

5. Mix solidified freon with a metal rod to liquefy it again (**Figure 3E**).
6. Grip the outer ring of the copper carrier with tweezers and immerse it into cooled freon with a gentle shaking of tweezers for 8 s (**Figure 3F**). After 8 s, quickly transfer the carrier into another Dewar flask filled with LN₂.
7. Proceed immediately with fracturing or storing the samples in LN₂. In the latter case, mark a cryovial and cool the vial and tweezer tips by submerging them into LN₂ (**Figure 3G**). Under LN₂, collect frozen copper carriers into the vial, close it, and store them in the LN₂ container (**Figure 3H**) until freeze fracturing.

3. Fracturing of EVs and making the replicas

NOTE: Prepare the freeze-fracturing unit according to the manufacturer's operating instructions. (**Figure 4A**). Clean the chamber of the unit. Position platinum (Pt/C) and carbon (C) guns at angles of 45° and 90°, respectively (**Figure 4B**).

1. Start the unit vacuum system. When pressure of 6.6×10^{-2} Pa (5×10^{-4} Torr) is reached, cool down the unit chamber to -150 °C.
2. Transfer the copper carriers with frozen samples into a freeze-fracturing unit using dry tweezers (**Figure 4C**). Use cryotransfer or work fast to avoid thawing the sample and deposition of the ice crystals. Secure the carriers onto the sample table.
3. Wait until the vacuum reaches again 6.6×10^{-2} Pa (5×10^{-4} Torr), and then set the knife temperature to -100 °C (**Figure 4D**).

4. Wait until the vacuum reaches 1.0×10^{-3} Pa (8×10^{-6} Torr).
5. Observe the sample with binoculars and carefully approach the knife (**Figure 4E**).
6. Begin sectioning the sample by turning on the motorized movement of the knife (**Figure 4F**) and section until the surface of the sample is smooth (**Figure 4G**).
7. For fracturing, turn off the motorized movement of the knife and proceed with slow manual control of the knife, thereby fracturing the sample (**Figure 4H**). In order to protect the fractured surface from forming ice crystals and debris until shadowing, move the knife above the fractured sample.
8. Proceed with the Pt shadowing at 45° (**Figure 4I, J**).
 1. Prepare a stopwatch and/or turn on the quartz crystal monitor on the freeze-fracturing unit, which will allow supervision of the thickness of the Pt on the sample. The recommended thickness of the Pt layer as measured on the quartz crystal monitor is 2.5 nm, which corresponds to 4 s of shadowing at a given high tension and current (i.e., the speed of Pt shadowing is 0.63 nm/s).
 2. Before starting the shadowing, move the knife away from the sample. Apply high tension on the Pt/C gun (1,600 V), and increase the current to 60 mA. Sparks of Pt should appear and should begin to shadow the sample. At this point, start the 4 s countdown and/or observe and locate the position of Pt on the quartz crystal monitor.

NOTE: The recommended thickness of the C layer is 2.5 nm, which corresponds to 10 s of shadowing at a given high tension and current.

3. Turn off the current and high tension when the desired thickness of Pt is obtained.
9. Proceed with the C shadowing at 90° (i.e., the speed of C shadowing is 0.25 nm/s).
 1. Apply high tension on the C gun (1,900 V), increase the current to 90 mA, and sparks of C should appear and begin to shadow the sample; at that moment, start the 10 s countdown. Turn off the current and high tension when the desired thickness of C is obtained.
5. Use a TEM microscope to image the replicas and obtain micrographs.
 1. To do so, insert a TEM grid with a replica and start the TEM imaging according to the manufacturer's operating manuals. Work at 80 kV or 100 kV.
6. Inspect the sample and acquire micrographs at lower and higher magnifications with a camera on TEM.
7. Analyze the micrographs of the MVs. For measurements of the MV diameters, use Fiji/ImageJ software¹⁶. The diameter of MVs is $4/\pi$ times the measurement on the micrographs according to Hallett et al.¹⁷.

4. Cleaning the replicas and replica analysis

1. Use the copper carriers from the sample table and transfer them with tweezers to distilled water at room temperature in a porcelain 12-well plate (**Figure 4K**). The replicas will float on the water surface, while the carriers sink (**Figure 4L**).
2. Transfer the replicas with a wire loop from distilled water into a well with sodium hypochlorite. Cover and leave overnight at room temperature in a fume hood.

CAUTION: Sodium hypochlorite is toxic. Work in a fume hood, wear protective gloves, and discard them appropriately.
3. Transfer the replicas to ddH₂O and wash for 30 min. Repeat 3 times.
4. Transfer the replicas with a wire loop to a mesh copper TEM grid (e.g., square or honeycomb 100+ mesh). Air dry the grids for 2 h, and then store them in a grid storage box until microscopy.

NOTE: Generally, grids can be stored for months in dark, dry, room temperature conditions.

Representative Results

MVs were isolated from the conditioned medium of cancer urothelial T24 cells after differential centrifugations. Following the protocol, the EV fraction was first detected after centrifugation at 10,000 × *g* when it was seen as a white pellet (**Figure 2G**).

Next, the EVs were processed according to the above protocol and examined under TEM. Pt/C shadowing produced (**Figure 4L**) relatively large replicas that frequently broke up into smaller fragments during the cleaning step. Large replicas and their smaller fragments were picked on the TEM grid and compared under the microscope. The results showed no differences in the quality of the replica surfaces regardless of their size, and they can, therefore, all be used. Low magnification examinations showed regions of the replica with i) a homogeneous surface (background), ii) concave and convex spherical profiles (vesicles), and iii) regions of damaged surface (artifacts; **Figure 5A**). Typical artifacts were seen as ruptures, folds, and irregular dimmer shadows (i.e., replicas of ice-crystal deposits on the specimen). It is also

important to note that no cell debris or cellular organelles were seen, confirming the purity of the sample (**Figure 5B**).

The isolated vesicles were commonly gathered either in clusters of three or more or were individually distributed (**Figure 5B**). The vesicles were spherical, which points to good preservation of the ultrastructure during isolation, fixation, and freezing (**Figure 5C**). "Flat-ball" and elongated vesicles (**Figure 5C**), which were seen occasionally, were presumably artifacts of preparation and were not included in the subsequent measurements of vesicle diameter. The diameter of the visible profiles was 238.5 nm (± 8.0 nm, $n = 190$), which, taking into account the correction factor proposed by Hallett et al.¹⁷, corresponds to the mean vesicle diameter of 304 nm (± 10 nm; **Figure 5D**). The size correlates to a diameter range of MVs between 100 nm and 1000 nm and proves the effectiveness of the used isolation protocol. The

images of the vesicles together with diameter determination unequivocally confirmed that the EVs in the isolate were enriched with MVs.

The analysis of the replicas revealed the organization of P-face and E-face of the MV limiting membranes. MVs were observed as concave and convex round shapes (**Figure 5C,E,F**), reflecting the fracture plane. The convex shapes represent E-faces (i.e., fractured exoplasmic leaflet of the membranes; **Figure 5E**). The exoplasmic faces of the EVs had a smooth, uniform appearance. The concave shapes correspond to P-faces (**Figure 5F**). In the P-faces, a few protruding intramembrane particles were seen within smooth membranes (**Figure 5C,F**). This implies that MVs isolated from cancer urothelial T24 cells contain only a low amount of membrane proteins.

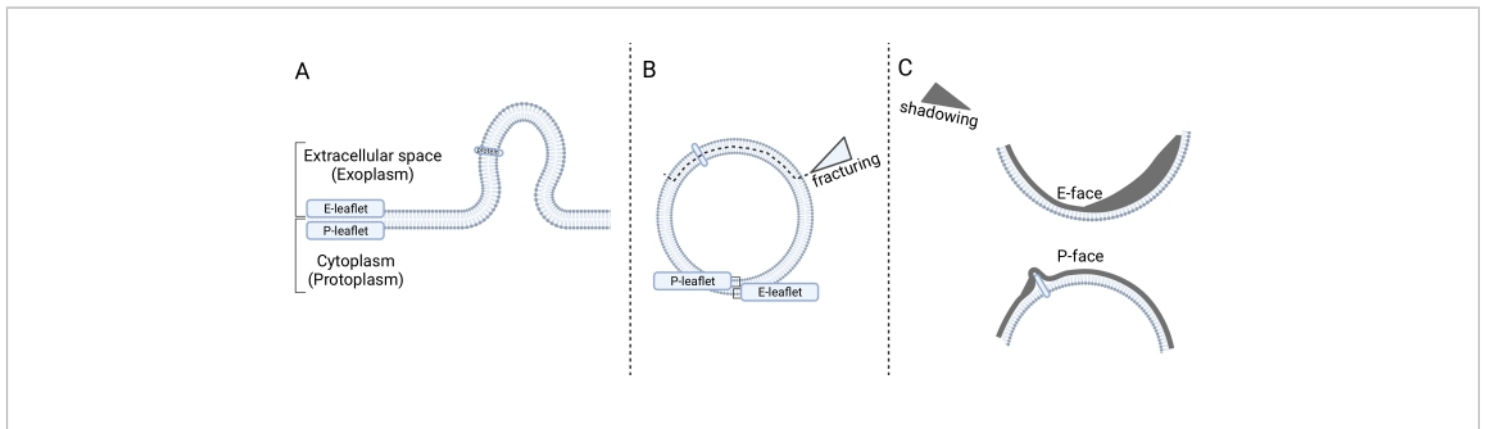


Figure 1: Schematic presentation of membrane determination after freeze-fracturing. (A) Microvesicles bud from the plasma membrane into the extracellular space. (B) Microvesicle is limited with P- and E- membrane leaflet until freeze-fracturing, which splits the leaflets and exposes the interior views of leaflets, termed fractured faces. (C) After Pt/C shadowing, two fractured faces are discernible: the protoplasmic face (P-face) with a convex shape facing the cytoplasm (protoplasm) and an exoplasmic face (E-face) with a concave shape facing the extracellular space. **Figure 1** was created using Biorender.com. [Please click here to view a larger version of this figure.](#)

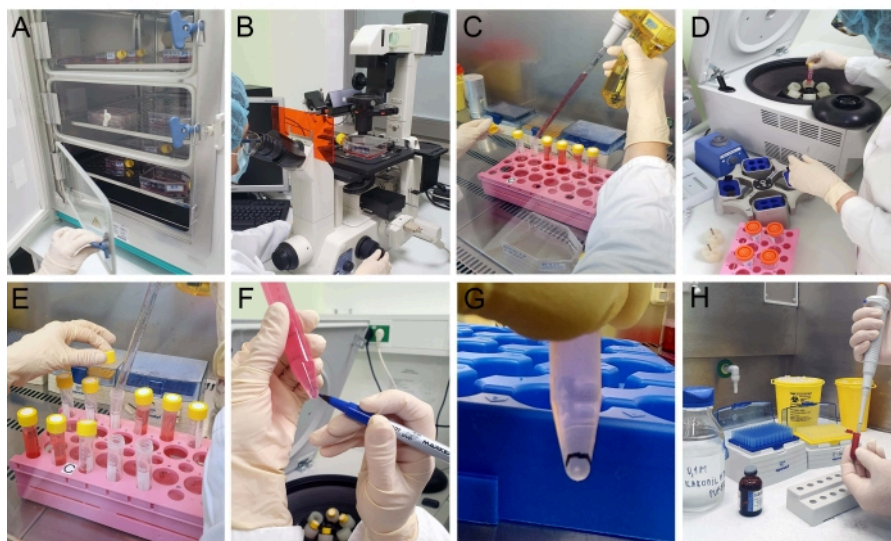


Figure 2: Isolation of EVs. (A) T24 cells grown in a CO₂ incubator are examined with (B) a light microscope to confirm their viability and confluence before MV isolation. (C) The cell culture medium is collected and (D) consecutively centrifuged at 300 × *g* and at 2,000 × *g* (E) each time the supernatant is collected. (F,G) After the centrifugation at 10,000 × *g*, a white patch indicating a pellet is visible and marked. The supernatant is removed and (H) fixative is carefully added to the pellet without resuspending it. [Please click here to view a larger version of this figure.](#)

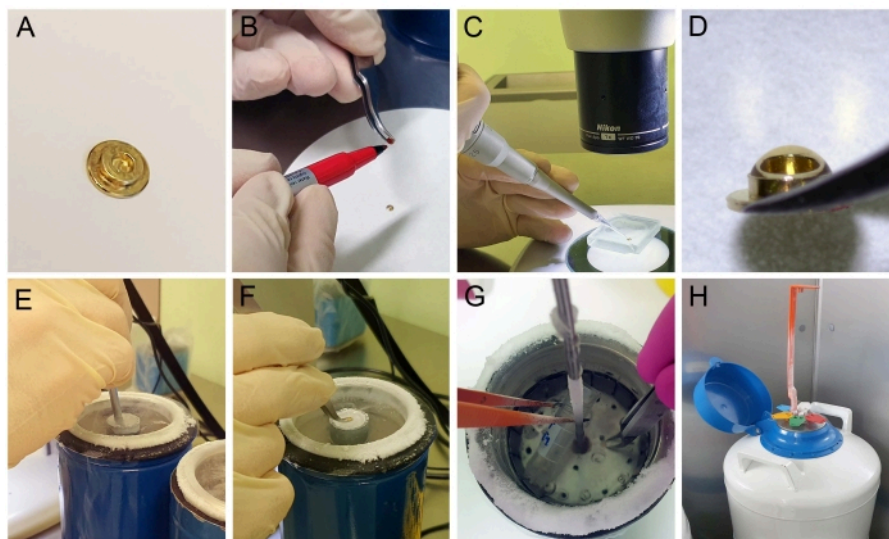


Figure 3: Freezing of EVs. (A) Air-dried clean copper carriers with a central pit are (B) marked before processing. Microvesicles are resuspended in glycerol to get a homogenous sample and (C) added to a central pit of a copper carrier under a stereomicroscope. (D) One has to add a volume of the sample such that it forms a convex drop in the central pit. (E) Immediately before freezing, mix LN₂-cooled freon with a metal rod to liquefy the freon. (F) Freeze the sample by submerging it in freon, and then (G) transfer it into LN₂. (H) Carriers with the frozen sample can be collected into cryovials and stored in an LN₂ Dewar container. [Please click here to view a larger version of this figure.](#)



Figure 4: Freeze-fracturing and making a replica. (A) Freeze-fracturing unit. Inside the unit chamber (B) is a platinum (Pt) and carbon (C) electron gun, a knife, and the sample table. (C) To start fracturing, carriers with the sample are transferred to the sample table, (D) the freeze-fracturing unit is cooled, and a vacuum is established. (E) Sectioning is done by motorized (F) movement of the knife, but fracturing is preferably done manually. (G) Sample before sectioning and (H) after fracturing. (I) Immediately after fracturing, the replica is made. (J) During this process, Pt is shadowed on the sample. Platinum shadowing is seen as a bright light (sparks) in the chamber. (K) Sample carriers are collected into a porcelain well filled with

water. (L) Replica (arrow) floating in the sodium hypochlorite solution during the cleaning step. [Please click here to view a larger version of this figure.](#)

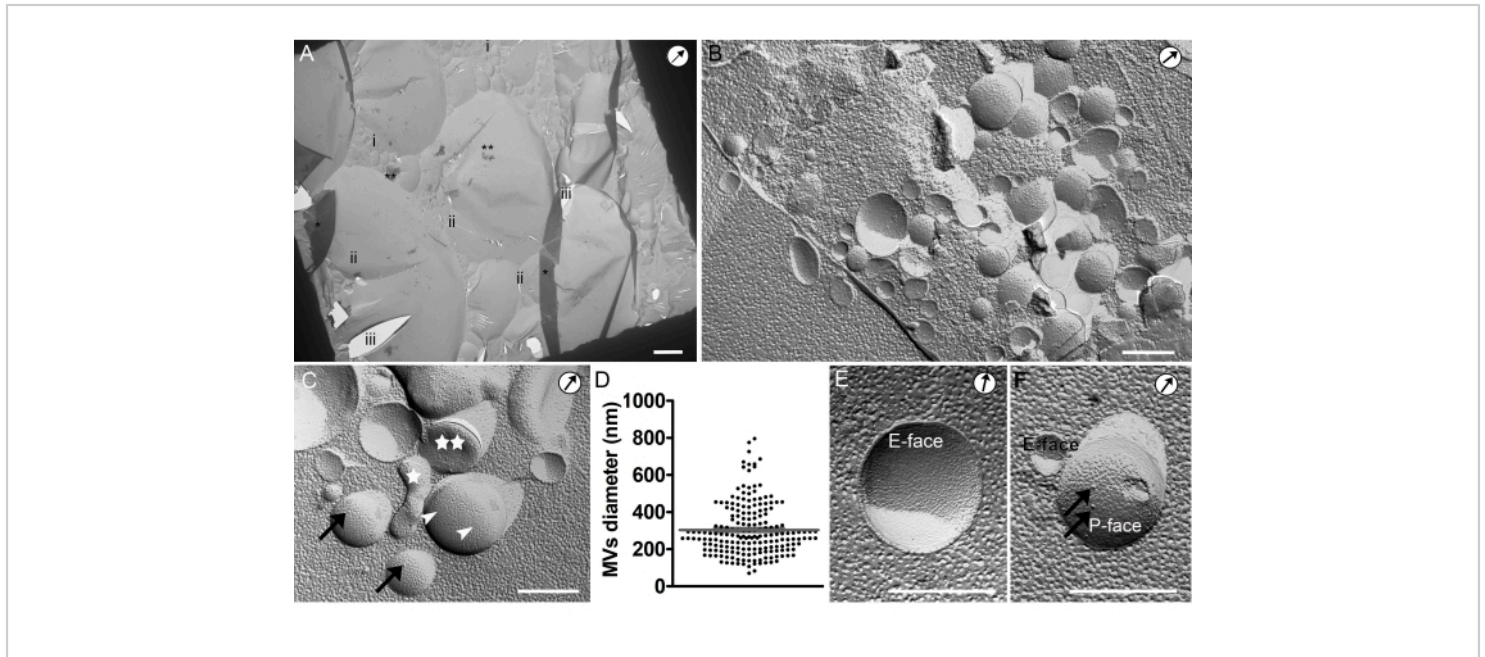


Figure 5: Electron micrographs of freeze-fractured and Pt/C shadowed MVs. (A) An overview of the freeze-fractured and shadowed EV pellet (i) at lower magnification. The homogeneous surface is background (ii), bright areas are ruptures in the replicas (iii), darker areas are folds of replicas (asterisk), and irregular dimmer shadows are due to ice crystals (two asterisks). (B) Cluster of round-shaped EVs with concave and convex surfaces. (C) High magnification of EVs. In convex fractures, which exhibit P-face of the EV membranes, intramembrane particles (arrows) and patches of a smooth surface (arrowheads) are seen. Extracellular vesicles with elongated (star) and flat-ball shapes (two stars) are found. (D) The mean diameter of isolated urothelial MVs is $304 \text{ nm} \pm 10 \text{ nm}$ according to the size measurements as proposed by Hallett et al.¹⁷. Data are presented as mean \pm SEM. (E,F) E-face and P-face of MVs. Legend: arrows = intramembrane particles in P-face, encircled arrows = the direction of Pt/C shadowing. Scale bars: A = $10 \mu\text{m}$, B-F = 400 nm . [Please click here to view a larger version of this figure.](#)

Discussion

The characterization of MVs, or any other population of isolated EVs, is of prime importance to begin with before starting downstream analyses like "omics" studies or functional studies^{11,18}. Herein, EVs from human invasive bladder cancer urothelial T24 cells were isolated by centrifugation, and following the provided protocol for analysis

by freeze-fracture electron microscopy, we demonstrated that the isolated fraction was enriched in MVs^{11,13}. The isolate of MVs was devoid of cell debris or organelles, confirming a successful isolation and purification protocol.

The combination of chemical fixation and freezing, which are critical steps of the protocol, retained the spherical shape of the EVs¹². However, precautions are needed

when assessing EV diameter by freeze-fracturing¹⁷. Since the fracture passes through the sample randomly, MV membranes are split into their equatorial and non-equatorial planes. To provide a rigorous method for analyzing the images of freeze-fractured and shadowed specimens, Hallett et al. showed that the mean vesicle diameter is $4/\pi$ times the actual size of the vesicular diameter on the image¹⁷. Accounting for that, EVs from T24 cells were calculated to have a diameter of 304 nm, which fits in the MV's theoretical size distribution range of 100-1000 nm¹⁹.

Freeze-fracturing can supplement negative staining, the most extensively used TEM technique to visualize EVs. By negative staining, the sample is commonly chemically fixed, dried and attached to a TEM grid, and contrasted with uranyl solution. Without supporting media, EVs tend to collapse, which gives them a cup-shaped appearance. By freeze-fracturing, we show that MVs are spheres, which reflects their shape in extracellular spaces and body fluids¹². By that, our results are also in agreement with observations of EVs in cryo-ultrathin sections²⁰.

A crucial advantage of the freeze-fracture technique is its power to resolve the internal organization of the limiting membrane, which is a key factor in understanding how EVs are targeted to and interact with recipient membranes. Here, we analyzed the membranes of MVs, yet freeze-fracturing could reveal the membrane organization of any other population of EVs. MVs are formed by plasma membrane budding; therefore, plasma membrane proteins and protein clusters are expected to be found in the MV membrane. Our results supported that the MVs from T24 cells contained intramembrane particles, presenting integral membrane proteins. Based on particle distribution between the E-face and P-face, it is reasonable to expect

that the particles observed in MVs are transmembrane proteins uroplakins, which are urothelial cell specific^{21,24}. The observed particles were sparse, which is in accordance with previous studies reporting a reduction in uroplakins during urothelial carcinogenesis^{21,22,23}. However, to further investigate the protein composition of MV membranes, the use of the freeze-fracture replica immune-labeling (FRIL) technique is recommended. FRIL is an upgrade of the presented freeze-fracture technique and is dedicated to revealing the identity of proteins in replicas by antibody recognition^{24,25}. To sum up, the freeze-fracture technique is an electron microscopy technique suitable for the characterization of the EV limiting membrane, as well as the shape, size, and purity of the isolated EV fractions. The presented protocol can be used also for the assessment of other populations of isolated EVs; therefore, the freeze-fracturing technique merits inclusion in the International Society for Extracellular Vesicles guidelines for studies exploring the organization of EV limiting membranes.

Disclosures

The authors declare no conflicts of interest.

Acknowledgments

This research was funded by the Slovenian Research Agency (research core funding no. P3-0108 and project J7-2594) and the MRIC UL IP-0510 Infrastructure program. This work contributes to the COST Action CA17116 International Network for Translating Research on Perinatal Derivatives into Therapeutic Approaches (SPRINT), supported by COST (European Cooperation in Science and Technology). The authors would like to thank Linda Štrus, Sanja Čabraja, Nada Pavlica Dubarič, and Sabina Železnik for technical help with cell culturing and preparing the samples and Marko Vogrinc,

Ota Širca Roš, and Nejc Debevec for technical help preparing the video.

References

1. Raposo, G., Stoorvogel, W. Extracellular vesicles: Exosomes, microvesicles, and friends. *The Journal of Cell Biology*. **200** (4), 373-383 (2013).
2. Willms, E., Cabanas, C., Mager, I., Wood, M. J. A., Vader, P. Extracellular vesicle heterogeneity: Subpopulations, isolation techniques, and diverse functions in cancer progression. *Frontiers in Immunology*. **9**, 738 (2018).
3. van Niel, G., D'Angelo, G., Raposo, G. Shedding light on the cell biology of extracellular vesicles. *Nature Reviews Molecular Cell Biology*. **19**, 213-228 (2018).
4. Cocucci, E., Racchetti, G., Meldolesi, J. Shedding microvesicles: Artefacts no more. *Trends in Cell Biology*. **19** (2), 43-51 (2009).
5. Urabe, F. et al. Extracellular vesicles as biomarkers and therapeutic targets for cancer. *American Journal of Physiology-Cell Physiology*. **318** (1), C29-C39 (2020).
6. Tricarico, C., Clancy, J., D'Souza-Schorey, C. Biology and biogenesis of shed microvesicles. *Small GTPases*. **8** (4), 220-232 (2017).
7. Georgantzoglou, N., Pergaris, A., Masaoutis, C., Theocharis, S. Extracellular vesicles as biomarkers carriers in bladder cancer: Diagnosis, surveillance, and treatment. *International Journal of Molecular Sciences*. **22** (5), 2744 (2021).
8. Słomka, A., Urban, S. K., Lukacs-Kornek, V., Żekanowska, E., Kornek, M. Large extracellular vesicles: Have we found the holy grail of inflammation? *Frontiers in Immunology*. **9**, 2723 (2018).
9. Han, L., Lam, E. W. F., Sun, Y. Extracellular vesicles in the tumor microenvironment: Old stories, but new tales. *Molecular Cancer*. **18** (1), 59 (2019).
10. Muralidharan-Chari, V., Clancy, J. W., Sedgwick, A., D'Souza-Schorey, C. Microvesicles: Mediators of extracellular communication during cancer progression. *Journal of Cell Science*. **123** (Pt 10), 1603-1611 (2010).
11. Kowal, J. et al. Proteomic comparison defines novel markers to characterize heterogeneous populations of extracellular vesicle subtypes. *Proceedings of the National Academy of Sciences of the United States of America*. **113** (8), 968-977 (2016).
12. They, C., Amigorena, S., Raposo, G., Clayton, A. Isolation and characterization of exosomes from cell culture supernatants and biological fluids. *Current Protocols in Cell Biology*. **Chapter 3**, Unit 3.22 (2006).
13. They, C. et al. Minimal information for studies of extracellular vesicles 2018 (MISEV2018): A position statement of the International Society for Extracellular Vesicles and update of the MISEV2014 guidelines. *Journal of Extracellular Vesicles*. **7** (1), 1535750 (2018).
14. Severs, N. J. Freeze-fracture electron microscopy. *Nature Protocols*. **2** (3), 547-576 (2007).
15. Severs, N. J., Robenek, H. Freeze-fracture cytochemistry in cell biology. *Methods in Cell Biology*. **88**, 181-186 (2008).
16. Rueden, C. T. et al. ImageJ2: ImageJ for the next generation of scientific image data. *BMC Bioinformatics*. **18**(1), 529 (2017).
17. Hallett, F. R., Nickel, B., Samuels, C., Krygsman, P. H. Determination of vesicle size distributions by

- freeze-fracture electron microscopy. *Journal of Electron Microscopy*. **17** (4), 459-466 (1991).
18. Nigro, A. et al. Selective loss of microvesicles is a major issue of the differential centrifugation isolation protocols. *Scientific Reports*. **11**, 3589 (2021).
 19. Szatanek, R. et al. The methods of choice for extracellular vesicles (EVs) characterization. *International Journal of Molecular Sciences*. **18** (6), 1153 (2017).
 20. Iliev, D. et al. Stimulation of exosome release by extracellular DNA is conserved across multiple cell types. *The FEBS Journal*. **285** (16), 3114-3133 (2018).
 21. Zupančič, D., Zakrajšek, M., Zhou, G., Romih, R. Expression and localization of four uroplakins in urothelial preneoplastic lesions. *Histochemistry and Cell Biology*. **136** (4), 491-500 (2011).
 22. Wu, X. R., Manabe, M., Yu, J., Sun, T. T. Large scale purification and immunolocalization of bovine uroplakins I, II, and III. Molecular markers of urothelial differentiation. *The Journal of Biological Chemistry*. **265** (31), 19170-19179 (1990).
 23. Kreft, M. E., Hudoklin, S., Jezernik, K., Romih, R. Formation and maintenance of blood-urine barrier in urothelium. *Protoplasma*. **246** (1-4), 3-14 (2010).
 24. Kreft, M. E., Robenek, H. Freeze-fracture replica immunolabelling reveals urothelial plaques in cultured urothelial cells. *PLoS One*. **7** (6), e38509 (2012).
 25. Robenek, H. et al. Topography of lipid droplet-associated proteins: Insights from freeze-fracture replica immunogold labeling. *Journal of Lipids*. **2011**, 409371 (2011).